THE UTILIZATION OF VOLCANO ENERGY.

JOHN L. COLP
AUGUSTINE S. FURUMOTO EDITORS

PROCEEDINGS OF A CONFERENCE,

~~HELD AT~~

HILO, HAWAII,

~~ON~~

FEBRUARY 4-8, 1974.

CO-SPONSORED BY
UNITED STATES NATIONAL SCIENCE FOUNDATION
JAPAN SOCIETY FOR THE PROMOTION OF SCIENCE

Foci of Volcanoes

By Izumi YOKOYAMA

Department of Geophysics, Faculty of Science,

Hokkaido University

One may assume a centre of volcanic activities beneath the edifice of an active volcano, which is here called the focus of the volcano. Sometimes it may be a " magma reservoir ". Its depth may differ with types of magma and change with time. In this paper, foci of volcanoes are discussed from the viewpoints of four items.

1. Geomagnetic changes related with volcanic activities

The researches of the changes in geomagnetic field related with volcanic eruptions as well as those with earthquakes have been one of the aims of the geomagnetic surveys throughout Japan which were commenced by A. TANAKADATE in 1893. Many observational data accumulated since that time have given a large effect on the images of physical mechanisms and energetics of volcanic activities in this country. At the time of the 1940 great eruption of Miyake Volcano, a few geophysicists observed the anomalous changes in geomagnetic field independently each other. These observations convinced Japanese geophysicists that the geomagnetic changes accompanied by volcanic activities might be expected on basaltic volcanoes such as Miyake and Oosima Volcanoes, Izu.

DISCLAIMER

On the occasion of the 1950 great eruption of Oosima Volcano, Rikitake (1951) made the geomagnetic studies at its early stage: from the observations of the changes in magnetic dip, he deduced that a spherical part of about 2 km in diameter at a depth of about 5.5 km beneath the volcano was heated above the Curie temperature and lost its magnetization. Since 1951, a continuous observation of the changes in geomagnetic declination has been made at a point on the western coast of Oosima Island in order to detect the relation between volcanic activities and geomagnetic changes. This observation point is deemed adequate for the purpose because declination there is expected to be prone to change in connection with the changes of magnetization of the volcano as seen from the distribution of declination on Oosima shown in Fig. 1. The magnetometer which has a magnet suspended with a fine phosphor-bronze ribbon is installed in a cave. The semi-monthly means obtained from hourly values and from daily means successively are plotted in Fig. 2. In the figure, also the active periods of the volcano are shown by the columns, but the 1950-51 eruption was very large comparing with the other activities: about 5×10^7 ton of lavas were erupted by this eruption and about 1×10^6 ton of lavas by the 1953-54 eruption. In the figure, the differences between Oosima and Kakioka Magnetic Observatory which is situated at a distance of 180 km north-east from Oosima, are obtained in order to eliminate the effects of geomagnetic disturbances of outer origin. Declination at Oosima has changed eastward after the climax of the eruption in 1951, repeating small oscillatory changes and reached asymptotically a certain level about 1957. The double cir-

cles in Fig. 2 denote the semi-monthly means which are calibrated by the absolute observations by means of a G. S. I. (Geographical Survey Institute) type magnetometer. From this figure, it may be concluded that the declination at the western coast changed gradually about 7 minutes of arc eastward for 6 years 1951 to 1957 as the aftereffects of the 1950-51 eruption. Taking into consideration the difference of the rate of the secular changes in declination between Oosima and Kakioka, i.e. 0.25 and 0.15 minutes of arc per year for 1950 and 1960 respectively according to the G. S. I., we may say that the anomalous change amounted about 5.5 minutes of arc per 6 years.

If the changes in geomagnetic field during 1951 to 1957 is approximated by a dipole field, its moment and depth can be determined by the results of the continuous observation of declination and the temporary ones of dip on Oosima. Thus, the depth of the dipole is estimated at $1 \sim 2$ km and the increase in moment as the order of 3×10^{13} emu. As already discussed by the present author (1967), the magnetic dipole which approximates the geomagnetic anomalies observed on Oosima Volcano, is situated at a depth of about 2 km below sea level at the centre of the island and has the moment of about 7.1×10^{14} emu. The above dipole interpreting the anomalous changes for 6 years , is about 4 % in moment of that corresponding to the geomagnetic anomaly there.

In the following, a possible cooling process to interpret the observed increase in dipole moment will be discussed: If we assume that the normal temperature at a depth of $1 \sim 2$ km beneath this volcano is 150°C and it had been elevated not so much, say by 100°C by 1951 when the activities were highest, and it recovered to

the almost normal stage after 6 years as the activities declined, the rocks there would restore magnetization about 2×10^{-2} emu/g according to the result of the measurement of the Oosima lavas by Nagata (1951). If we substitute the above dipole by a sphere in the sense of a very rough approximation, its radius is 0.9 km and its volume amounts to 3×10^{15} cc. This volume is very large as compared with that of the overflowed lavas (about 2×10^{13} cc) but the magma which intruded into the fissures in the sphere might be not so voluminous. And its actual shape may be rather oblate vertically along the conduits and its position is approximately the same to that of the dipole interpreting the geomagnetic anomalies on Oosima Volcano as shown in Fig. 3 which was proposed by the author (1969) as a schematic structure of the volcano. Taking density and specific heat of the lavas as 2.5 g/cc and 0.2 cal/g$^{\circ}$C respectively, we get the total heat necessary to change the mean temperature of the lavas by 100°C as about 1.5×10^{17} cal.

The activities of magma beneath the volcano would be highest almost at the same time as the highest surface activities in 1950 or 1951. For 6 years after the climax of the eruptions, the mean temperature of the lavas at that part might have recovered by nearly 100°C. The molten magma which had filled the vents and fissures in the spherical part at the most active period, overflowed to the earth surface or retreated back to the depth and hence, the heat source of high temperature has diminished in accordance with the decline of the activities. The temperature might have decreased by 100°C for 6 years not only by heat conduction but by steam emission; the most probable heat source of low temperature at a depth

of 1 ~ 2 km must be meteoric water. At Oosima Island, it rains about 300 cm in a year. If we assume that the rain water within the caldera (about 10 km^2 in area) contacts with the lavas and evaporates, the heat absorbed for 6 years amounts to about 1.1 X 10^{17} cal. This is approximately equal to the heat required for the cooling process as before-mentioned. The evaporated water partly expands through the crater into the air as volcanic clouds. Though a more quantitative discussion of the above cooling process is not impossible, it will be not completely successful because it necessarily needs a few assumptions concerning the concrete structures and physical conditions beneath the volcano. Thus, it may be safely said that the mean temperature of the spherical part corresponding to the dipole could be lowered by 100°C in 6 years.

In a summary, the geomagnetic changes related with the activities of Oosima Volcano are interpretable by the possible thermal processes at about 2 km deep beneath the volcano.

2. Crustal deformations related with volcanic activities

Crustal deformations associated with great eruptions of both basaltic and andesitic volcanoes have proved to be elastic as a rough approximation, and deformation analyses on some volcanoes such as Hawaii and Sakurazima have given some clue to the processes of the volcanic activities and their subsurface structure.

In order to interpret the crustal deformations observed around volcanoes, already MOGI (1958) presented a model of pressure

source of explosive or implosive types. On the other hand, the author (1971), for the same purpose, proposed an alternative model with pressure source of thrust type. The former model has pressure distribution expressed in spherical harmonics P_o^o (cos θ) and reminds us of magma reservoirs while the latter has P_1^o (cos θ) distribution symbolizing the points of dikes. The deformations of the semi-infinite elastic body caused by an internal pressure source of both types were already calculated by YAMAKAWA (1955) and SOEDA (1944) respectively. The displacement curves of the two models shown in Fig. 4 are not substantially different from each other. However, the vertical displacements of the surface right above the sources depend upon 3/4 (a^3/f^2) and 5/6 (a^2/F) respectively, where a denotes radius of the source sphere, f and F depths of the pressure sources of both the types. If we take $f = F = 10a$ and the other conditions remain the same, the latter is about 10 times larger than the former: In other words, to cause the same vertical displacements, P_1^o model needs the source pressure only one tenth of P_0^o model.

By curve-fitting to the observed vertical displacements in Fig. 4, the depths of the pressure sources can be determined. And also the distributions of horizontal displacements enable us to estimate approximately the depths of the pressure sources as the radial distances where the horizontal displacements take maxima.

Whether one adopts P_o^o model or P_1^o model, one must prefer a single model to superposed plural models because the mutual effects of the plural boundary conditions are not always negligible in the latter case.

Example 1: the 1914 eruption of Sakurazima, Japan

The remarkable depression around Sakurazima in its 1914 eruption is shown in Fig. 5. Mogi (1958) interpreted this depression by a model of P_o^o type and got the depth of pressure source as 10 km assuming the maximum depression to amount to 150 cm at point A in Fig. 5. The author (1971) applied a model of P_1^o type to the above depression and obtained the depth of pressure source as 6 km. In Fig. 6 the degrees of fitness of both the theoretical curves for the observed values are almost indiscriminate.

The pressure change at the source is determinable when the vertical displacement at the surface right above the pressure source and the depth of the source $\underset{\sim}{f}$ or $\underset{\sim}{F}$ are known. For the P_o^o model with $\underset{\sim}{f} = 1\underset{\sim}{0a} = 10$ km and 10^{11} c.g.s. as rigidity of the crust, the pressure change amounts to 20 Kbar. For the P_1^o model with $\underset{\sim}{F} = 1\underset{\sim}{0a} = 6$ km and the same rigidity as the above, the pressure change is 3 Kbar. On the other hand, the pressure of explosion of Sakurazima may be approximately estimated by the maximum horizontal arrival distance of the projected fragments. Strong showers of projected incandescent stones, dragging behind them threads or tails of grey vapors, like meteors, are said to have fallen hot, abundantly and hissing into the sea to a distance of $3 \sim 3.5$ km from the vent. Hence, the initial velocity is estimated at 170 m/sec., and the pressure of explosion as about 300 bar. The difference between the estimation by P_1^o model (3 Kbar) and that of the explosion pressure (300 bar) may not be unreasonable.

The horizontal displacements of the triangulation points on

and around Sakurazima during the period 1898 to 1914 after its eruption are shown in Fig. 7 where line AA denotes the fissure line with craterlets and ellipse BB does the convergent area of the displacement vectors which is indentical with the centre of depression found by the precise levels along Kagosima Bay shown in Fig. 5. As mentioned before, one may estimate the depth of pressure source at about 3 km beneath the volcano from the displacements at both sides of fissure line AA. Though the fissure already appeared at the earth surface and therefore, strictly speaking, the elastic theories are not appicable, the range of maximum horizontal displacements may be approximately determinable from the result of triangulation.

Example 2: the 1967-68 eruption of Kilauea, Hawaii

The 1967-68 eruption of Kilauea was discussed by FISKE and KINOSHITA (1969) from the standpoint of geodetic observations. During the period January, 1966 to October, 1967, they repeated 14 surveys of level and tilt and 7 geodimeter surveys and found the migration of the centre of uplift as shown in Fig. 8, by determining the successive centres assuming the P_o^o models.

The migration of the centre of uplift may be the wandering of the upward thrusts in sills and dikes which are approximated by the P_1^o model better than P_o^o model. Two examples of the vertical displacements of bench marks around Kilauea for the periods January ~July, 1966 and August ~ October, 1967 are analyzed by the P_1^o models. The results are shown in Fig. 9 (a) and (b), respec-

tively, where the double circles denote the reference points. In both the cases, the depths of the pressure sources are obtained as 2 ~ 3 km beneath the respective points in Fig. 8. FISKE and KINOSHITA (1969) drew a highly stylized diagram of the Kilauea magma reservoir as shown in Fig. 10 where the reservoir would consist of dense sills and feeder dikes.

The pressure change at the source of the deformation during the period January ~ July, 1966 is estimated at 640 bar for a P_1^o model with $\underset{\sim}{F}$ = 2 km.

From the horizontal displacements of 20 geodimeter lines during the period Jan. 6 to Feb. 21, 1967, FISKE and KINOSHITA (1969) estimated the depth of the pressure source at 2 km which is equal to the results obtained from the vertical displacements in the above.

In a brief summary, the pressure sources causing crustal deformations at several volcanoes are located at the depths of 2 ~ 6 km.

3. Magma transfer through volcanoes

The idea of magma reservoirs is a necessity of a working hypothesis which interpret differentiation of magmas beneath volcanoes. The existence of magma reservoirs, the author thinks, has not been proved beyond a possibility of doubt in field studies though several papers have discussed it from the standpoints of attenuation and conversion of the seismic waves through magma res-

ervoirs. In this Section, this will be discussed by magma transfer through volcanoes, in other words, by dynamics of magma.

One may estimate the order of magnitude of energy release from a volcano, if the discharge rate of ejecta from the volcano is known by historical records or geological studies. To estimate energy transfer by knowing mass transfer, the following formulae are applied according to the types of ejecta:

essential lava:

$$E\ (\text{solid}) = M\ (\Delta T \times C + H)\ J$$
$$= M\ (\ 1000^{\circ}C \times 0.25\ \text{cal}/^{\circ}C + 50\ \text{cal}\ )\ J$$
$$= 1.2 \times 10^{10}\ M\ (\ g\ )\ \text{erg},$$

where M denotes mass, T temperature difference, C specific heat, H latent heat, and J heat equivalent. Volatile material contained in lavas, which is almost all water vapour and amounts to 5 % in weight, also carries thermal energy:

$$E\ (\text{water}) = M_W\ (\Delta T \times C_W + H_W)\ J$$
$$= M \times 0.05\ (\ 900^{\circ}C \times 0.5\ \text{cal}/^{\circ}C + 639\ \text{cal}\ )\ J$$
$$= 0.2 \times 10^{10}\ M\ (\ g\ )\ \text{erg}.$$

Adding both the energies, we adopt the following formula:

$$E\ (\text{lava}) = 1.4 \times 10^{10}\ M\ (\ g\ )\ \text{erg},$$

pyroclastics (fragmentary ejecta):

$$E\ (\text{frag.}) = M\ (\Delta T \times C)\ J$$
$$= M\ (\ 500^{\circ}C \times 0.20\ \text{cal}/^{\circ}C\ )\ J$$
$$= 0.4 \times 10^{10}\ M\ (\ g\ )\ \text{erg}.$$

In the following discussion, all volcanic ejecta are classified into lavas and pyroclastics, and energy releases by them will be calculated by the above formulae. In other words, the energies

mean thermal ones transferred by ejecta and are proportional to the masses of the ejecta.

Example 1: Oosima.

One may refer to the historical records of the eruptions of this volcano up to the 7th century but these records are neither complete nor quantitative. NAKAMURA (1964) estimated volume of the ejecta at each period since 500 A.D. by laborious stratigraphical studies: He made the calculations on the basis of the distribution maps of twelve members, which comprise two elements, i.e., isopach contours of the fall deposits and distribution of lava-flows and scoria cones. Applying the same formulae as previous to the volume of each ejecta, he got the release rate of thermal energy as shown by the twelve steps in Fig. 11. Roughly speaking, the figure may represent that the volcano has constantly released energy at a rate of about 6×10^{24} erg/100 years during these 1500 years or since the caldera formation; exactly speaking, the respective rate of energy release at each period in the figure remains unknown. In Fig. 11, since 1876, energy releases are far smaller than former; NAKAMURA (1964) referred to them as follows: these eruptions may probably be regarded as a mere episode rather than a part of constructive activity in the long history of this volcano, but it may be possible that the mode of activity has changed after 1876.

According to the present principle, the energy transfer corresponds to the mass transfer; 8×10^{25} erg correspond to 6.2×10^{9} ton

during these 1500 years.

Example 2: Vesuvius.

G. IMBÒ (personal communication) has already investigated the volumes of ejecta at each period of the activities of Vesuvius since 1631. Referring the historical records, he classified the activities into the three types, i.e., lava effusion, pyroclastic explosion, and formation of cones in the craters (Strombolian type), and calculated the volumes of the ejecta precisely on the topographical maps. On the basis of his results, the rate of thermal energy release is obtained as shown in Fig. 12, where the right-hand ordinate approximately represents the corresponding mass.

The eruption in 1631 occurred after 490 years' quiescence and is not known well quantitatively. Therefore, the first step of large amount of energy release probably may be smoothed for a longer period. By a glance, the rate of energy release from Vesuvius seems constant since the middle of the 18th century to 1944. By a minute examination, it gradually increased since 1631 and attained the maximum and then has decreased asymptotically to zero. In fact, one shall be able to determine the recent tendency after accumulation of the future observations.

Summarizing the two features of energy release observed on Oosima and Vesuvius, one may get two schematic diagrams as shown in Fig. 13. At both the volcanoes, the respective chemical compositions of the lavas effused throughout the periods have shown little variation, which suggests that magma reservoirs, if any, have not

been emptied, but been under the same cycles of differentiation.

Fig. 13 (a) shows constant release of energy or mass as observed on Oosima, which means constant rate of magma supply to a volcano from the deep. Magma reservoirs, if any, beneath the volcano do not effect apparently the release of magma. A system of the volcano including magma reservoirs is stationary and therefore is open to the outside, or bigger sources such as the mantle.

Fig. 13 (b) shows a curve of energy release, of which rate takes a maximum and thereafter tends asymptotically to zero, as observed on Vesuvius. In an open system, entropy production rate depends mainly on the external supply, while in a closed system it tends to zero approaching equilibrium. In Fig. 13 (b) the former stage does not represent a closed system, but the latter stage is possible to represent a closed system. When once the system is closed, its rate of magma release to the craters depends on the residual volume in the reservoir, and consequently decreases with time. The present discussion is concerned with the closed system only. If one assumes that the latter stage in Fig. 13 (b) results from a closed system, one may estimate the initial condition of the system. In Fig. 12, at Vesuvius, the volcano system might be isolated from the deep in the beginning of the 19th century and afterwards it has been closed to the supply source. Since the period of isolation, the volcano has released about 1.6×10^9 m^3 of ejecta, which is equal to a sphere of about 1.5 km in diameter. This may represent the minimum volume of the magma reservoir which has formed a closed system: still it may hold residua and release them in future. Therefore the true volume of the reservoir may be larger

than the above value. In this interpretation, the magma reservoir can be replaced by a magma conduit.

Example 3: Kilauea, Hawaii

As for the magma supply rate at Kilauea Volcano, SWANSON (1972) denoted that the three longest eruptions lasting 4.5 months or longer during the period 1952 to 1971 produced lava at an overall constant rate of about 9×10^6 m^3 per month when recalculated on a nonvesicular basis and this eruption rate might represent the rate of magma supply from a deep source, probably the mantle.

To verify that this rate of supply from the mantle is essentially steady, he mentioned the following evidences: Noneruptive periods are typically characterized by swelling of Kilauea's summit area, which indicates storage of an increasingly large volume of magma and Kilauea's eruptions usually end when the summit is reinflating after initial deflation, which shows a continued movement of magma into Kilauea's conduit system.

4. Subsurface structure of calderas

Almost all the calderas in Japan, about 15 in number, have been surveyed gravimetrically by the author. The results of these surveys afford us a basis for quantitative discussion about the subsurface structure of the calderas and will improve our understanding of the mechanism of caldera formation. According to

the present author (1963), the calderas in Japan may be classified into two types from the standpoint of gravity anomaly: the calderas of a high gravity anomaly type such as Oosima (Fig. 14), associated with the effusive eruption of basaltic magma, to which Kilauea Caldera also belongs, and the calderas of a low gravity anomaly type such as Kuttyaro, Hakone and Aso, formed by explosive eruptions of siliceous magmas. In 1968, gravity surveys on the Krakatau Islands in the Sunda Straits and on Batur Caldera, Bali, were carried out by the author and D. HADIKUSUMO (1969): the former proved to be of the low gravity anomaly type and the latter of the high gravity anomaly type. As for the high gravity anomaly type, the present author (1969) already discussed the subsurface structure of Oosima. Therefore, in the following, the discussions will be confined to the low gravity anomaly type i.e., Kuttyaro and Sikotu Calderas in Hokkaido.

Example 1: Kuttyaro Caldera

Kuttyaro Caldera, measuring about 20 km in diameter, is one of the largest calderas in Japan; and its western half is a lake of which the average depth is about 40 m. Pumice which was ejected at the time of the catastrophe of the caldera formation (20 ~ 30,000 years B.P.) is fund widely spread around the caldera. A gravity survey on the surface of the frozen lake was carried out by the author (1958), and thereafter supplemented repeatedly.

The distribution of Bouguer anomalies on this caldera is shown in Fig. 15 where the dashed square contains about 100 gravity

points measured for prospecting in 1963. The gravity anomalies were already analyzed and a schematic profile of the subsurface structure of the caldera was presented by the author (1958) as shown in Fig. 16, where the density contrast ($\rho_0 - \rho_1$) was assumed to be 0.3 b/cc.

In 1963, a drilling 1000 m deep for developing steampower was made inside the caldera (at the centre of the dashed square in Fig. 15). NISHIDA and the author (1965) studied several physical properties of the cores from this drilling. Some of them, such as density and thermal conductivity, together with the distributions of temperature and heat flow value along the drilling, are shown in Fig. 17. At the drilling site, the depth of coarse material which is responsible for the observed gravity anomaly is expected to be less than 2 km as shown in Fig. 16. Therefore, almost all material to the depth of 1000 m must be coarse caldera deposits. In fact, there are many parts which consist of very coarse material as indicated by dots in the first column of Fig. 17. The majority of the cores are agglomerate tuff. Density increases from 1.7 to 2.2 g/cc with depth inside the caldera, while it may usually increase from 2.0 to 2.5 g/cc outside the caldera. Therefore, the before-mentioned density contrast 0.3 g/cc may be reasonable. As for the heat flow through the caldera, it is not continuous but it has a sink and a source: some heat may flow laterally at the two depths.

Example 2: Sikotu Caldera

Lake Sikotu is a caldera lake, measuring about 15 km in diameter and 368 m in its maximum depth. The bottom profile is of typical caldron shape. This caldera was formed in the Pleistocene: the age of carbonized wooden pieces found in the Sikotu welded tuff was determined by the radioactive method as about 18,000 years B.P. A gravimetric survey was carried out by means of a land gravimeter around the lake and a shipborne survey of total magnetic force was made on the lake in order to fill the gap in the gravity survey.

The distribution of Bouguer anomalies around the lake is shown in Fig. 18. In the eastern half of the lake, a residual positive anomaly in total magnetic force amounts to about 400 γ corresponding to a residual low gravity anomaly of about 20 mgal. The subsurface structure of Sikotu Caldera deduced from the results of the above surveys is schematically shown in Fig. 19 where also the structure of the eastern neighbouring district obtained by a seismic prospecting is shown. The basement (the Palaeozoic) in this district rises towards the east and is about 2 km deep beneath the caldera; and the depth of the caldera deposits is estimated at the same value. According to geological observations, one may find the Palaeozoic fragments in the pumice-flow deposits around the caldera. This means that the violent explosions might occur below this depth prior to the caldera formation.

In a summary, caldera bottoms are usually composed of fallbacks of caldera ejecta or post-caldera ejecta which cause low residual gravity anomalies. The depth of caldera deposits ranges 2~

4 km according to diameter of the calderas. At these depths, gigantic explosions might occur and a large amount of pumice and ash was extruded forming a circular conical depression.

In conclusion, it may be summarized that the foci of volcanoes are situated at the depths 2 $\sim$ 6 km beneath them and the sources of volcanic energies probably may be concentrated at these depths.

REFERENCES

Fiske, R. S. and W. T. Kinoshita, Inflation of Kilauea Volcano prior to its 1967-1968 eruption, Science, 165, 341-349, 1969.

Mogi, K., Relation between the eruptions of various volcanoes and the deformations of the ground surface around them, Bull. Earthq. Res. Inst., 36, 99-134, 1958.

Nagata, T., Magnetic properties of the lavas of Volcano Mihara (in Japanese), Journ. Geography (Tokyo), 60, 145-145, 1951.

Nakamura, K., Volcano-stratigraphic study of Oshima Volcano, Izu, Bull. Earthq. Res. Inst., 42, 649-728, 1964.

Nishida, Y. and I. Yokoyama, A note on physical properties of boring cores dug at Kuttyaro Caldera, Hokkaido (in Japanese). Geophys. Bull. Hokkaido Univ., 14, 53-58, 1965.

Rikitake, T., The distribution of magnetic dip in Ooshima Island and its change that accompanied the eruption of Volcano Mihara, 1950, Bull. Earthq. Res. Inst., 29, 161-181, 1951.

Soeda, K., On the deformations produced in a semi-infinite elastic solid by an interior source of stress (in Japanese), Quart. Jour. Seism., 13, 263-291, 1944.

Swanson, D. A., Magma supply rate at Kilauea Volcano, 1952-1971, Science, 175, 169-170, 1972.

Yamakawa, N., On the strain produced in a semi-infinite elastic solid by an interior source of stress (in Japanese), Jour. Seim. Soc. Japan, (ii) 8, 84-98, 1955.

Yokoyama, I., Geomagnetic anomaly on Volcanoes with relation to their subterranean structure, Bull. Earthq. Res. Inst., 35, 327-357, 1957.

Yokoyama, I., Gravity survey on Kuttyaro Caldera Lake. Jour. Phys. Earth, 6, 75-79, 1958.

Yokoyama, I., Structure of caldera and gravity anomaly. Bull. Volcanol., 26, 67-72, 1963.

Yokoyama, I. and M. Aota, Geophysical studies on Sikotu Caldera, Hokkaido, Japan, Jour. Fac. Sci., Hokkaido Univ., VII, 2, 103-122, 1965.

Yokoyama, I., The subsurface structure of Oosima Volcano, Izu, Jour. Phys. Earth, 17, 55-68, 1969.

Yokoyama, I. and D. HADIKUSUMO, Volcanological survey of Indonesian volcanoes, Part. 3. A gravity survey on the Krakatau Islands. Bull. Earthq. Res. Inst., 47, 991-1001, 1969.

Yokoyama, I., A model for the crustal deformation around volcanoes, Jour. Phys. Earth, 19, 199-207, 1971.

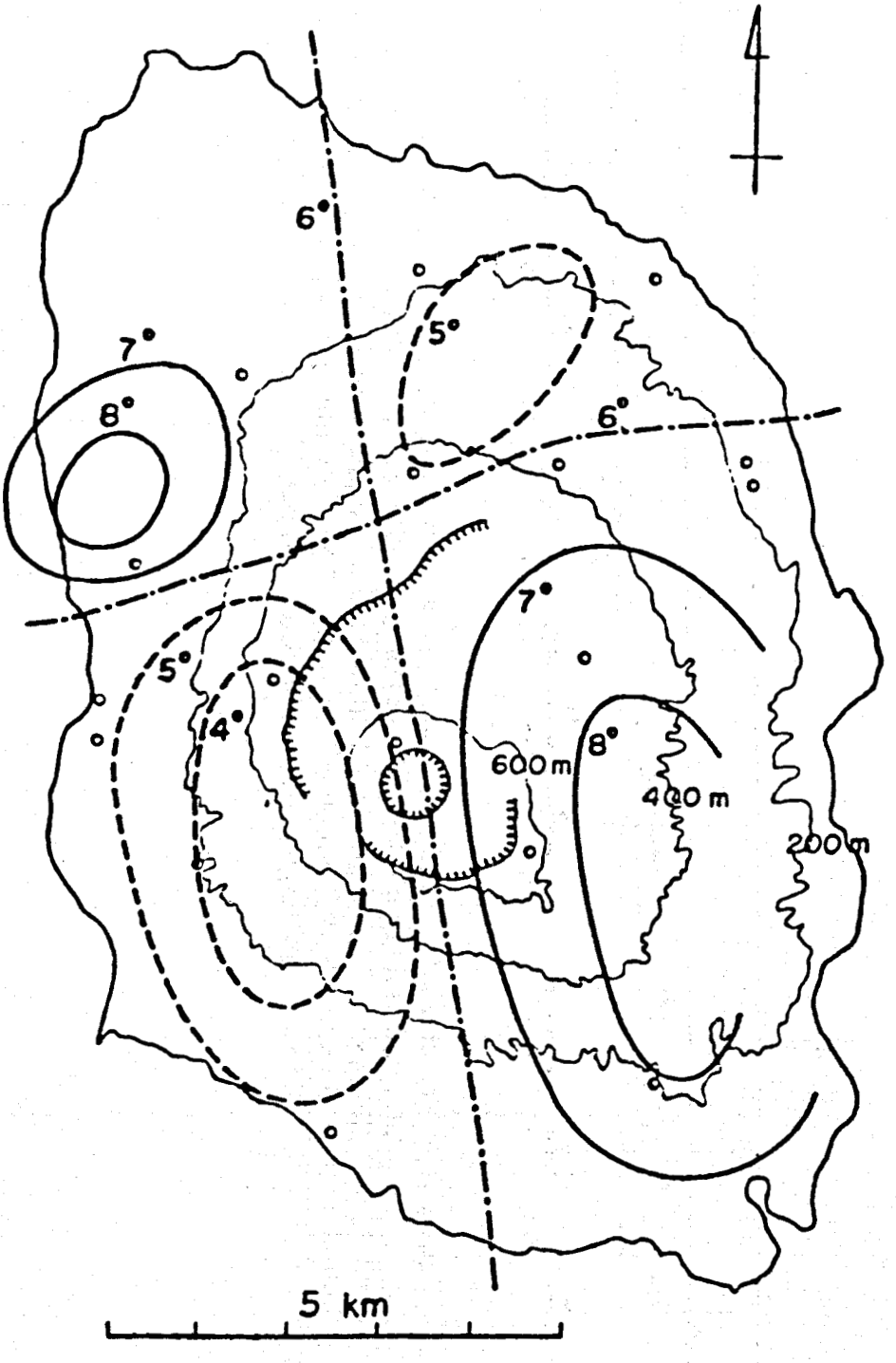

Figure 1. Distribution of the westerly declination for for 1956.0 on Oosima Island

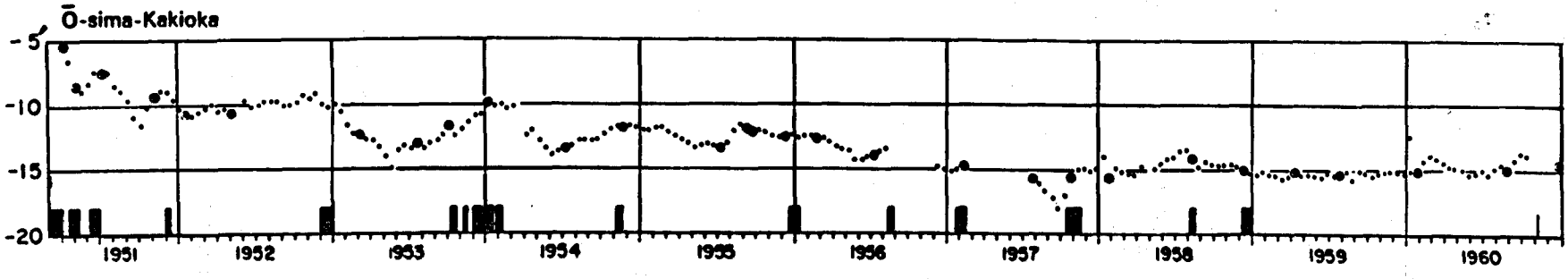

Figure 2. Variation of the difference of the semi-monthly mean of the westerly declination between Oosima and Kakioka. The encircled dots denote the values calibrated by absolute measurements. The columns denote the active periods of Oosima Volcano

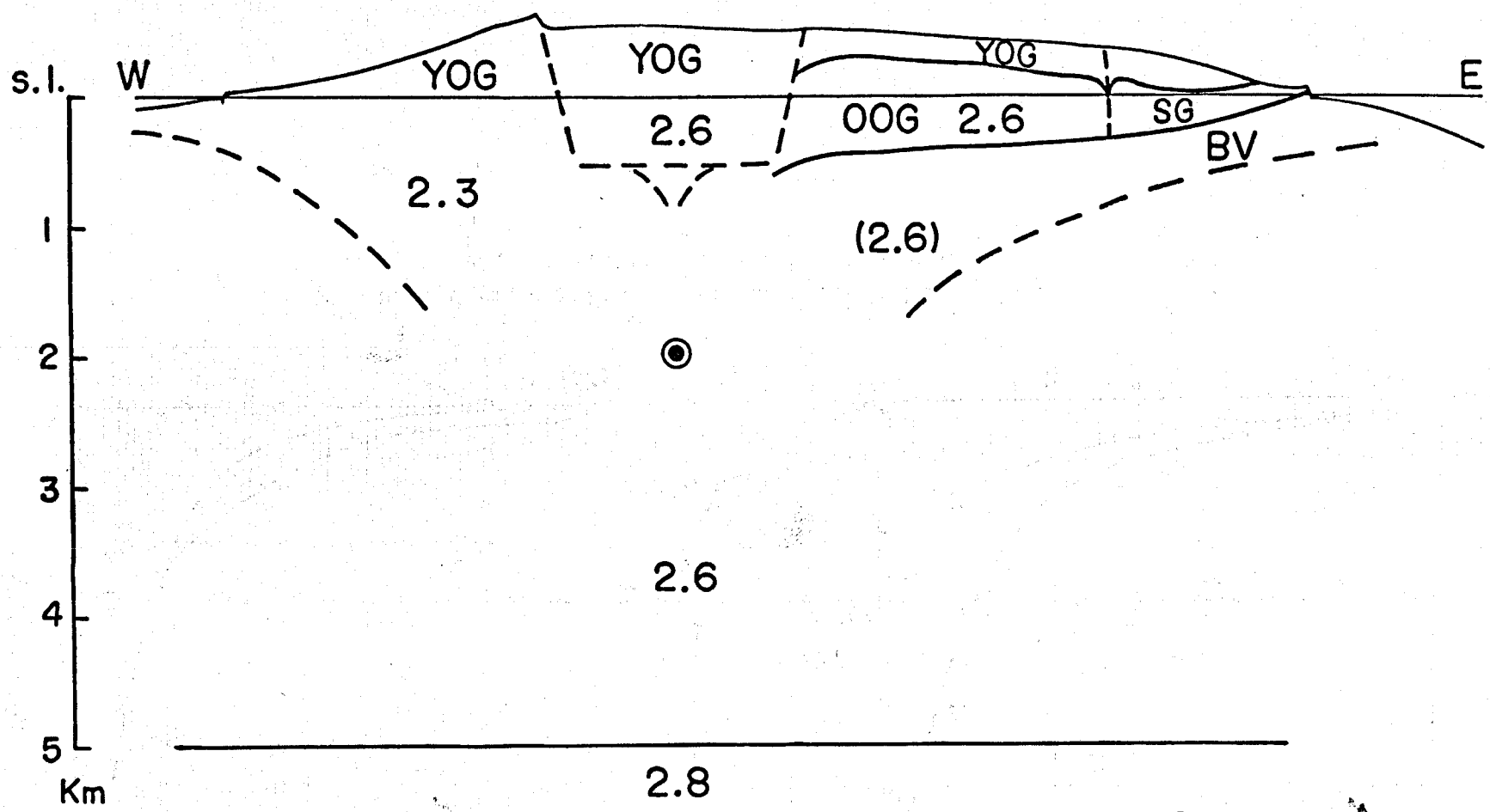

Figure 3. Schematic section of Oosima Volcano. The numerals denote density in g/cc and the double circle a dipole responsible for the geomagnetic anomalies.

YOG: Younger Oosima Group
OOG: Older Oosima Group
SG: Senzu Group (Miocene)
BV: Erosion remnant of basement volcanoes

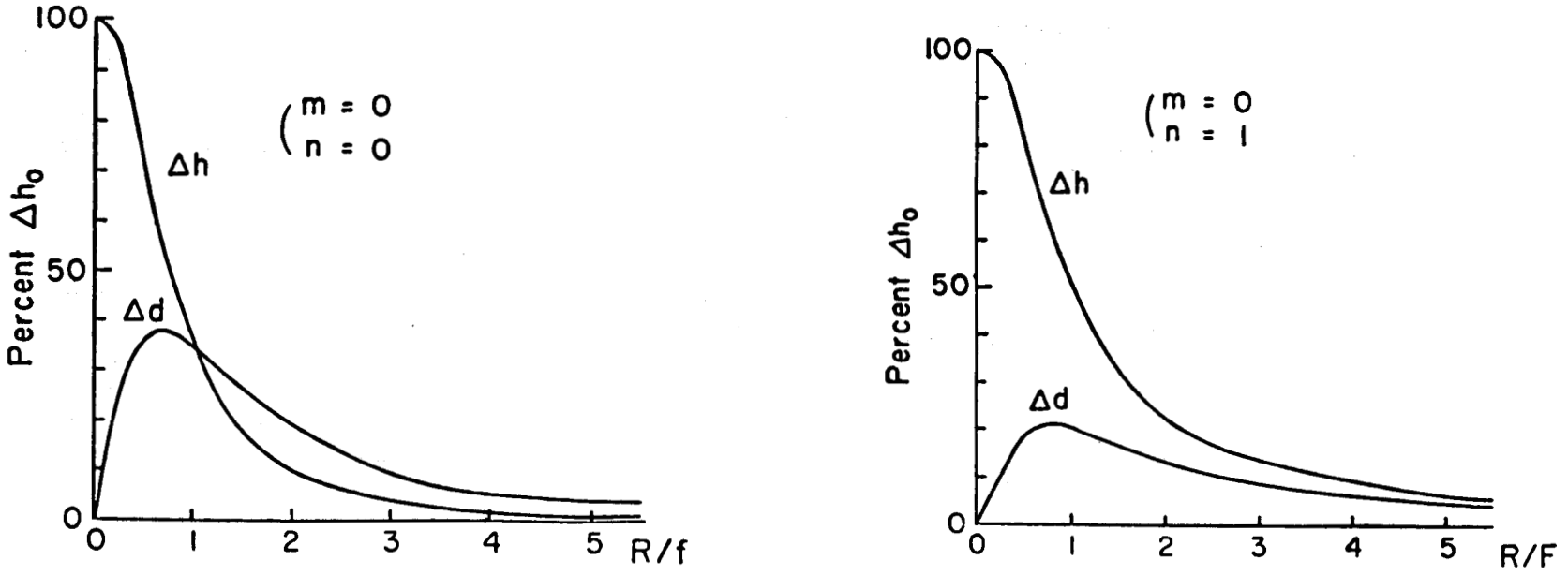

Figure 4. Vertical and radial displacements of the ground surface due to a pressure source of P_o^o or P_1^o type

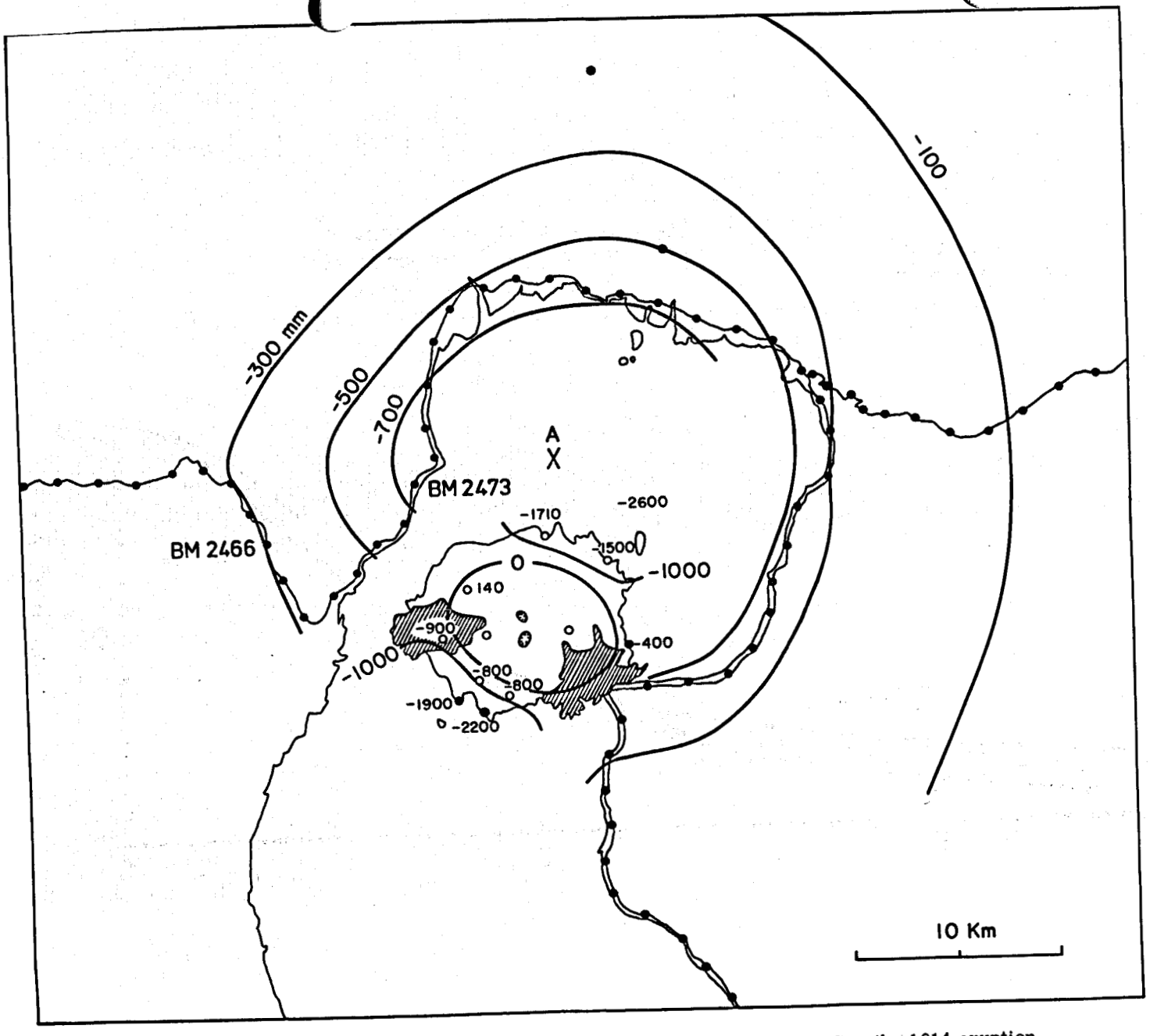

Figure 5. Vertical displacements around Sakurazima before and after the 1914 eruption (after F. Ōmori). A denotes the assumed centre of the depressions.

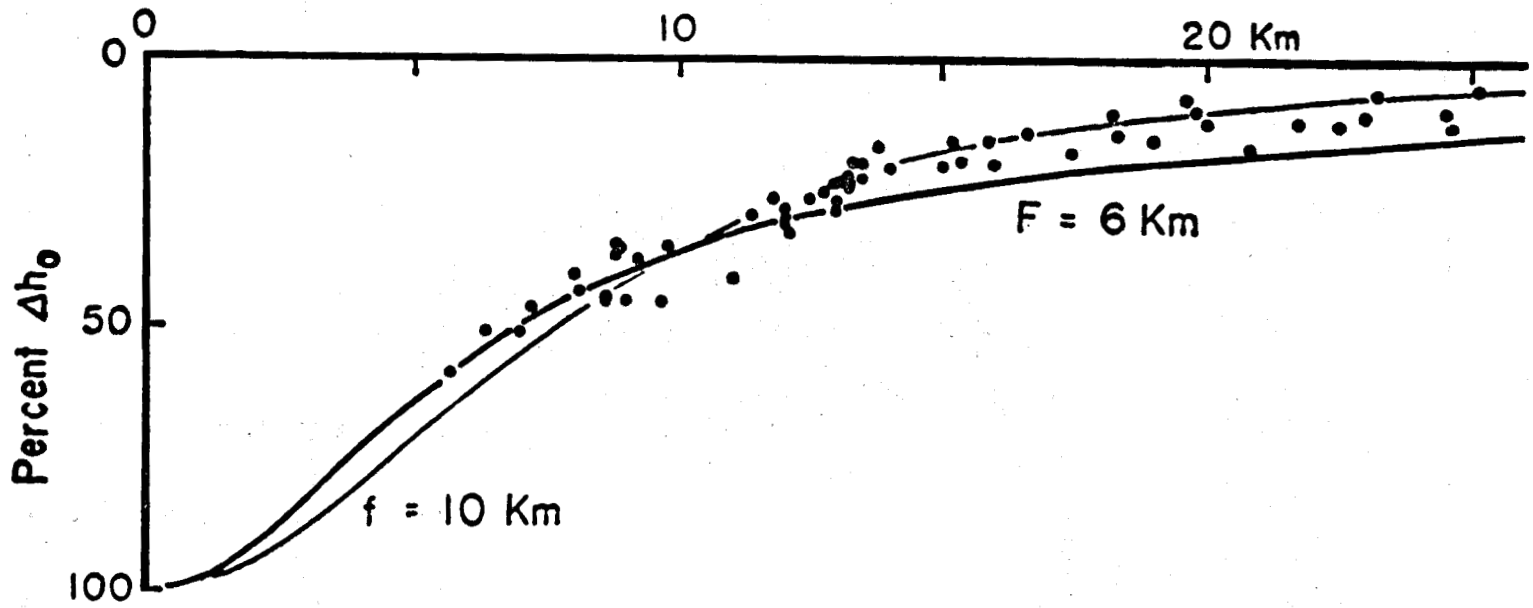

Figure 6. Radial distribution of the depressions observed before and after the 1914 eruption of Sakurazima and calculated by the two models. $\underset{\sim}{f}$ and $\underset{\sim}{F}$ denote the depths of the pressure sources of the P_o^o and P_1^o types respectively

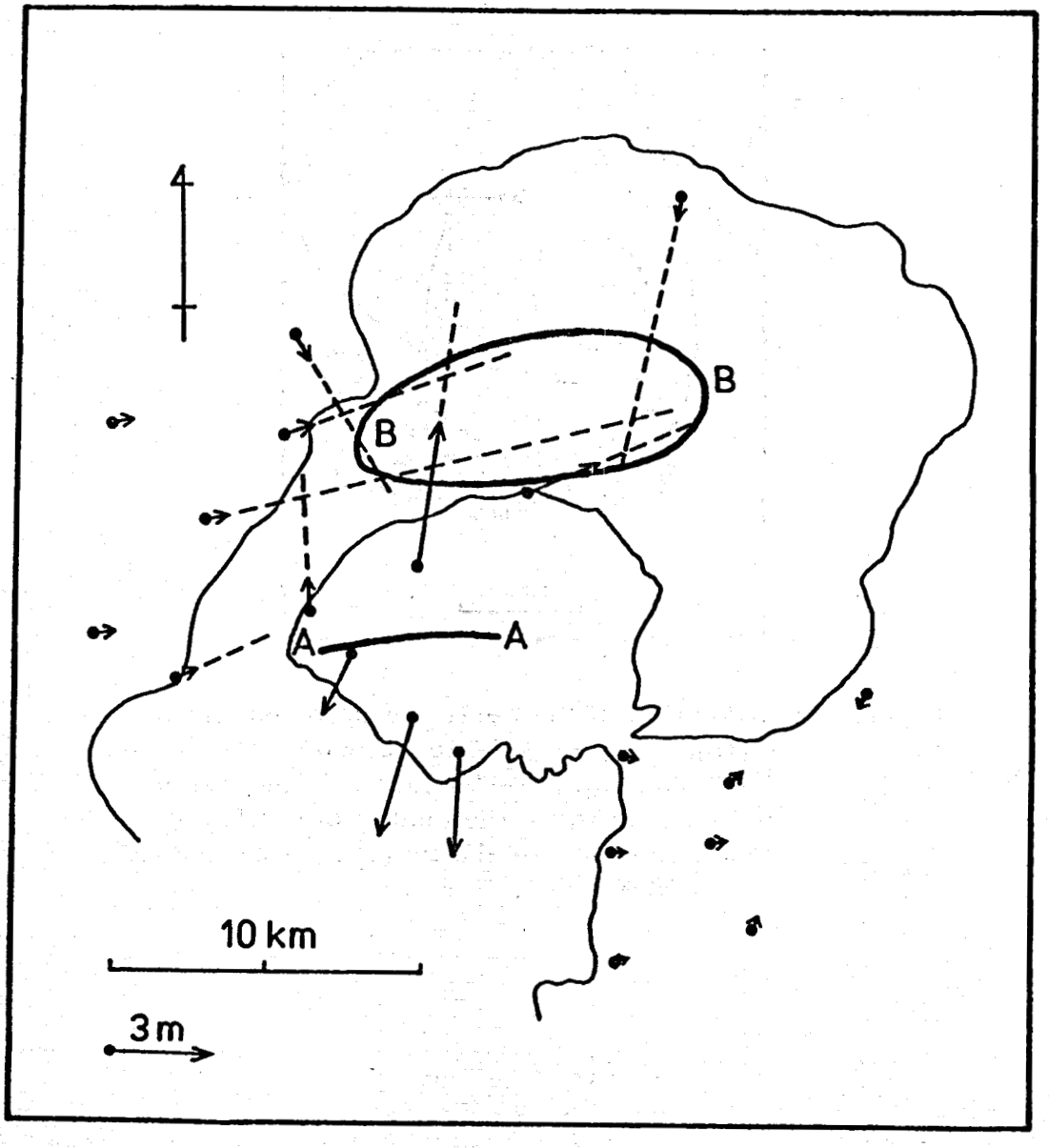

Figure 7. Horizontal displacements of triangulation points on Sakurazima and vicinity before and after its 1914 eruption. AA and BB denote the fissure line with craterlets and the depression centre respectively

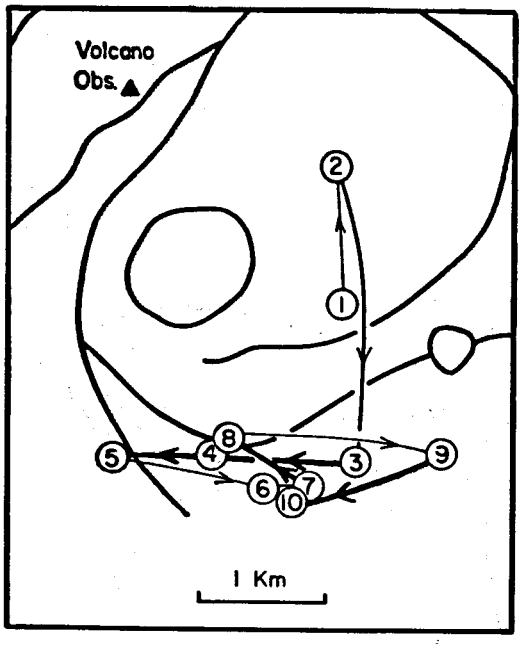

Figure 8. Migration of the centre of uplift observed during January 1966 to October 1967 in the 1967-68 eruption of Kilauea. Heary lines indicate shifts in the centre of uplift that took place in 2 weeks or less (after FISKE and KINOSHITA).

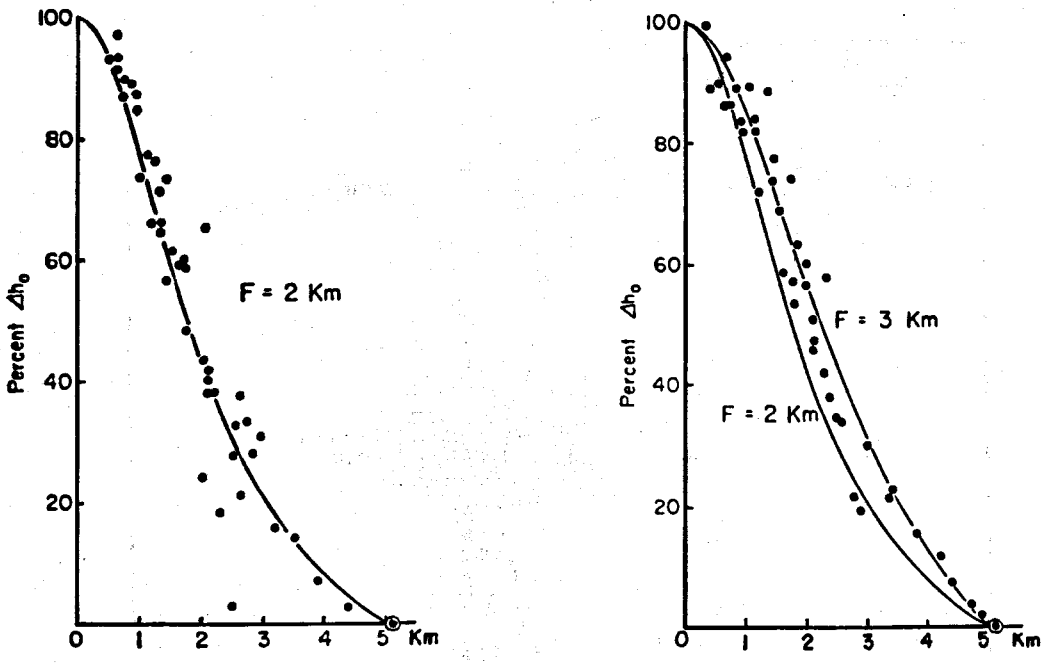

Figure 9. Radial distributions of the uplift observed in the 1967-68 eruption of Kilauea. The curves show the calculated ones by the P_1^Q models and the double circles do the reference points

a) January-July 1966, corresponding to ① in Figure 8,

b) August-October 1967, corresponding to ⑨ - ⑩ in Figure 8

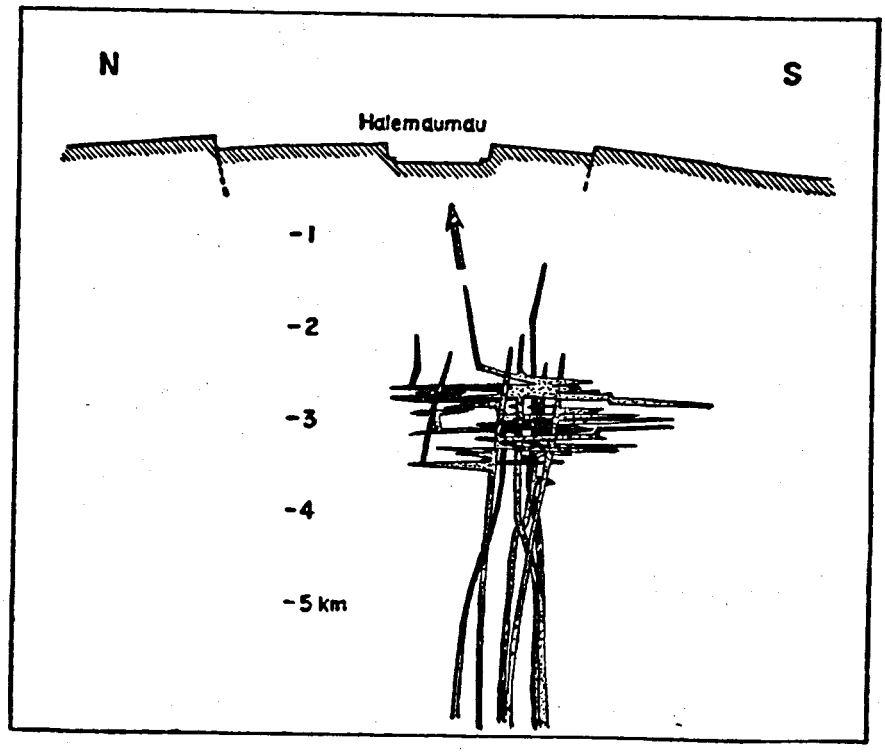

Figure 10. A highly stylized diagram of the Kilauea magma reservoir after FISKE and KINOSHITA

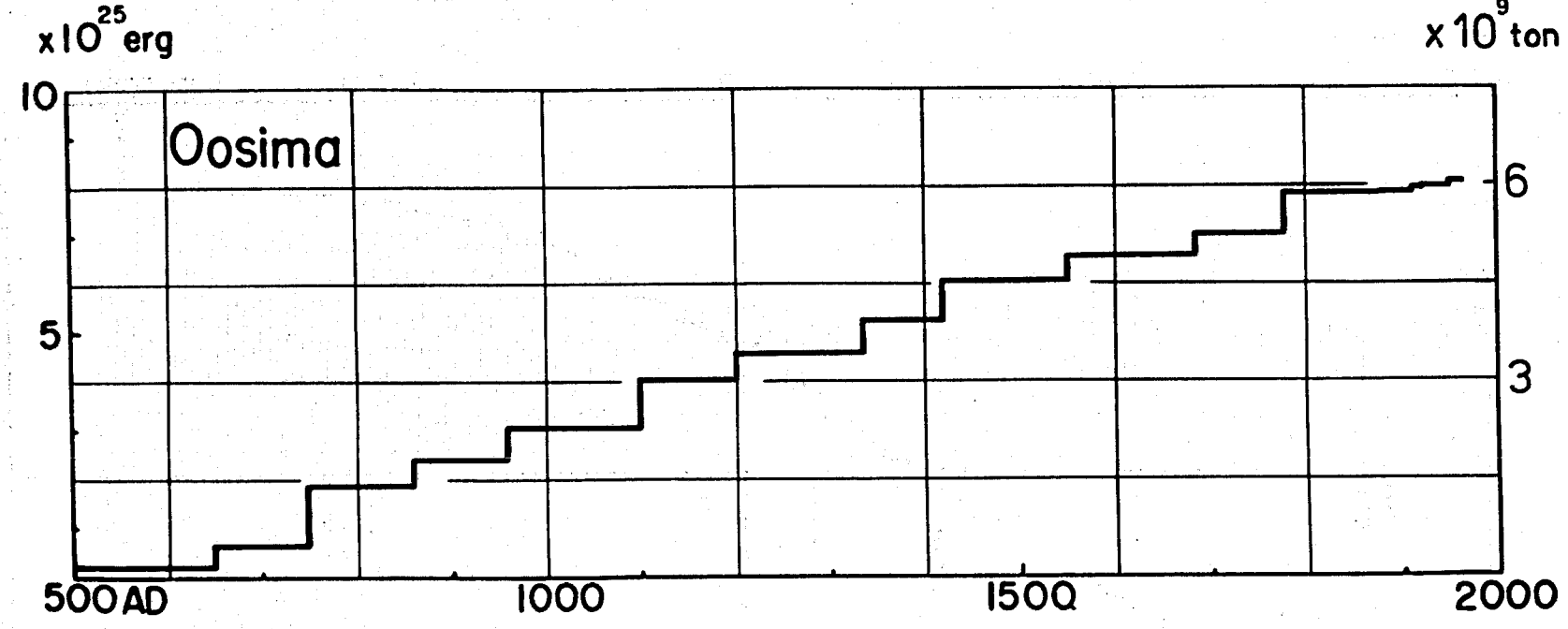

Figure 11. Cumulative energy release from Oosima since 500 A.D. after NAKAMURA

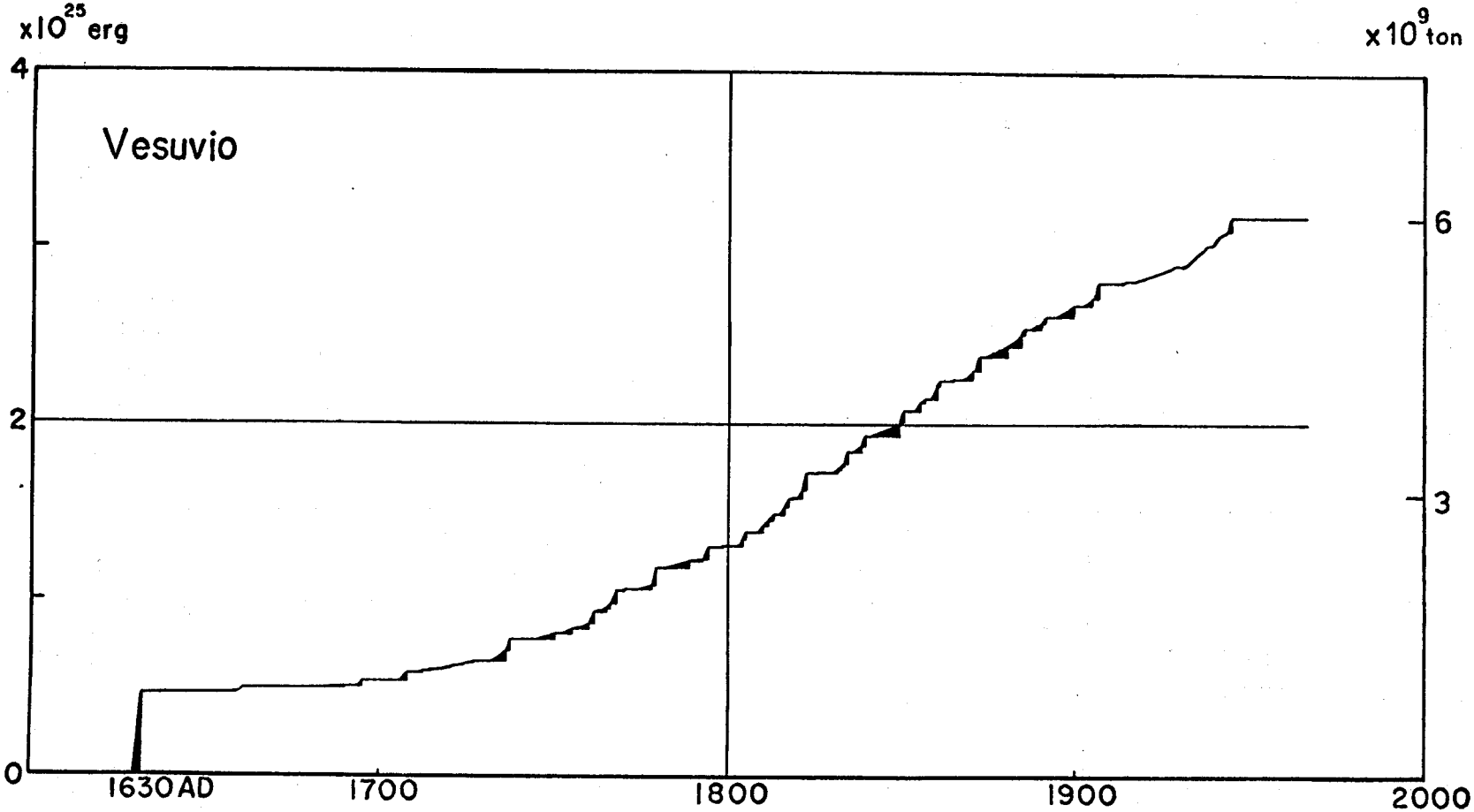

Figure 12. Cumulative energy release from Vesuvius since 1630 A.D. after G, Imbó (personal communication)

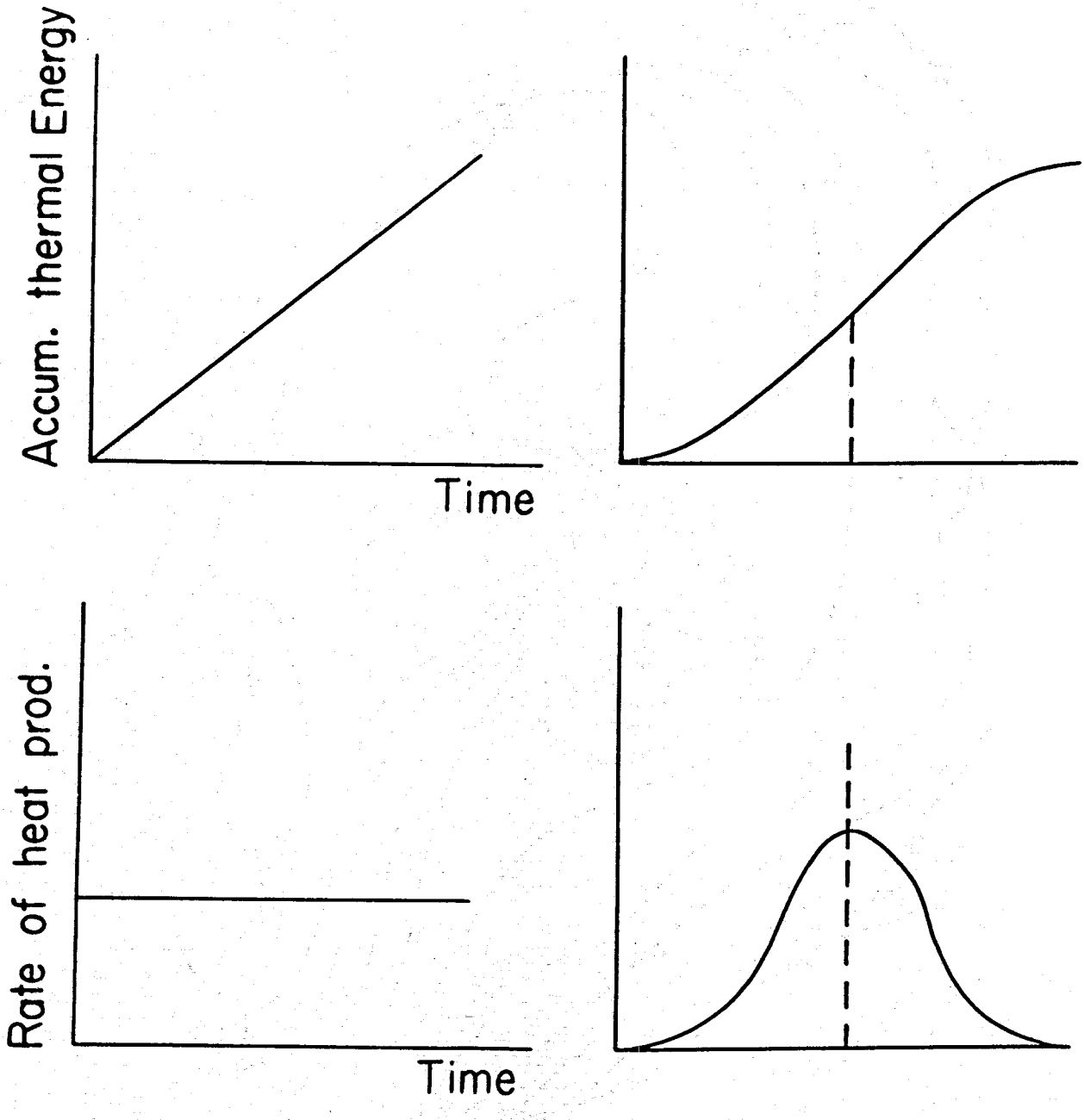

Figure 13. Schematic diagrams of cumulative energy release and rate of heat production from volcanoes

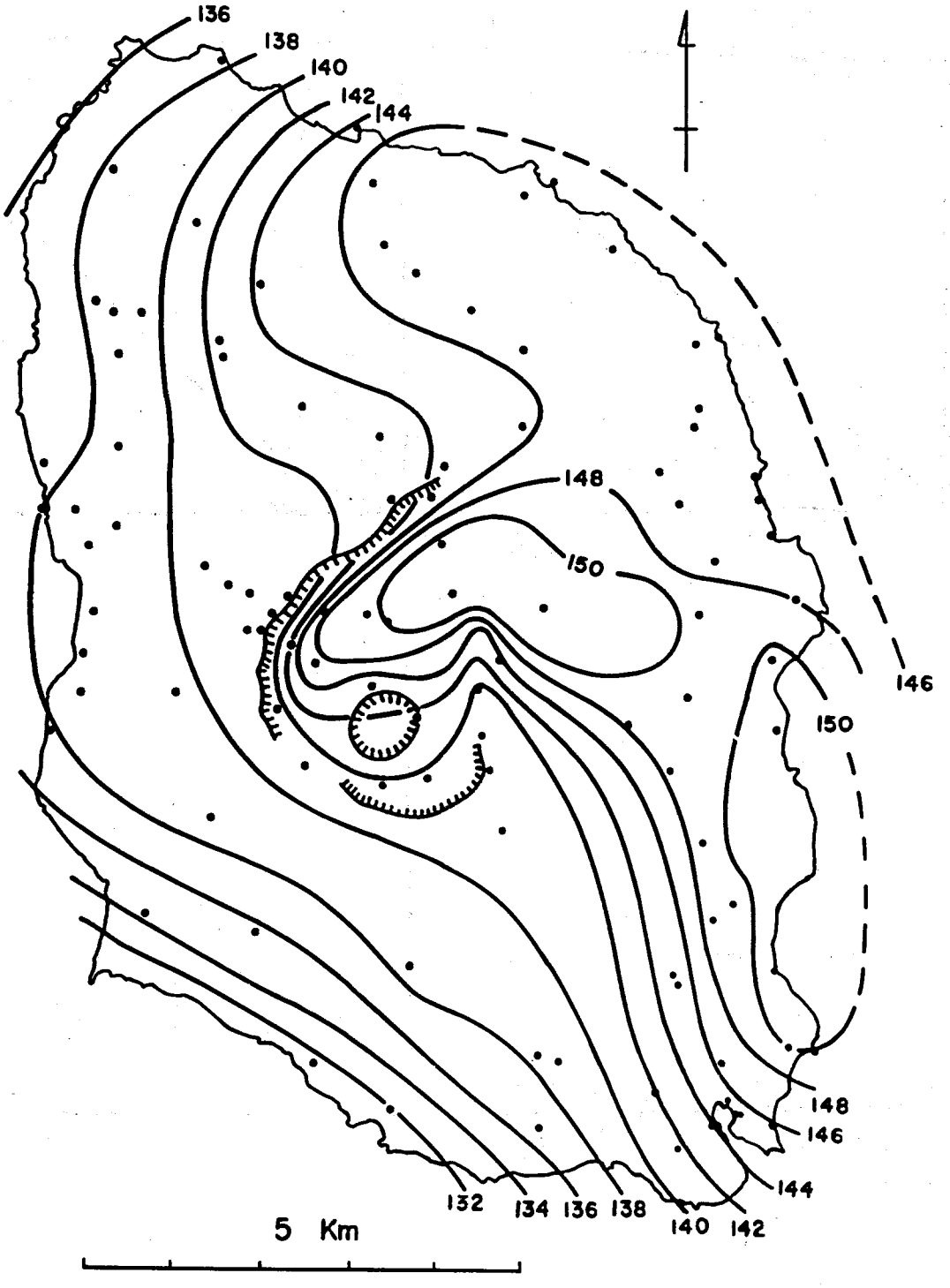

Figure 14. Distribution of Bouguer gravity anomalies on Oosima Volcano. Unit is mgal

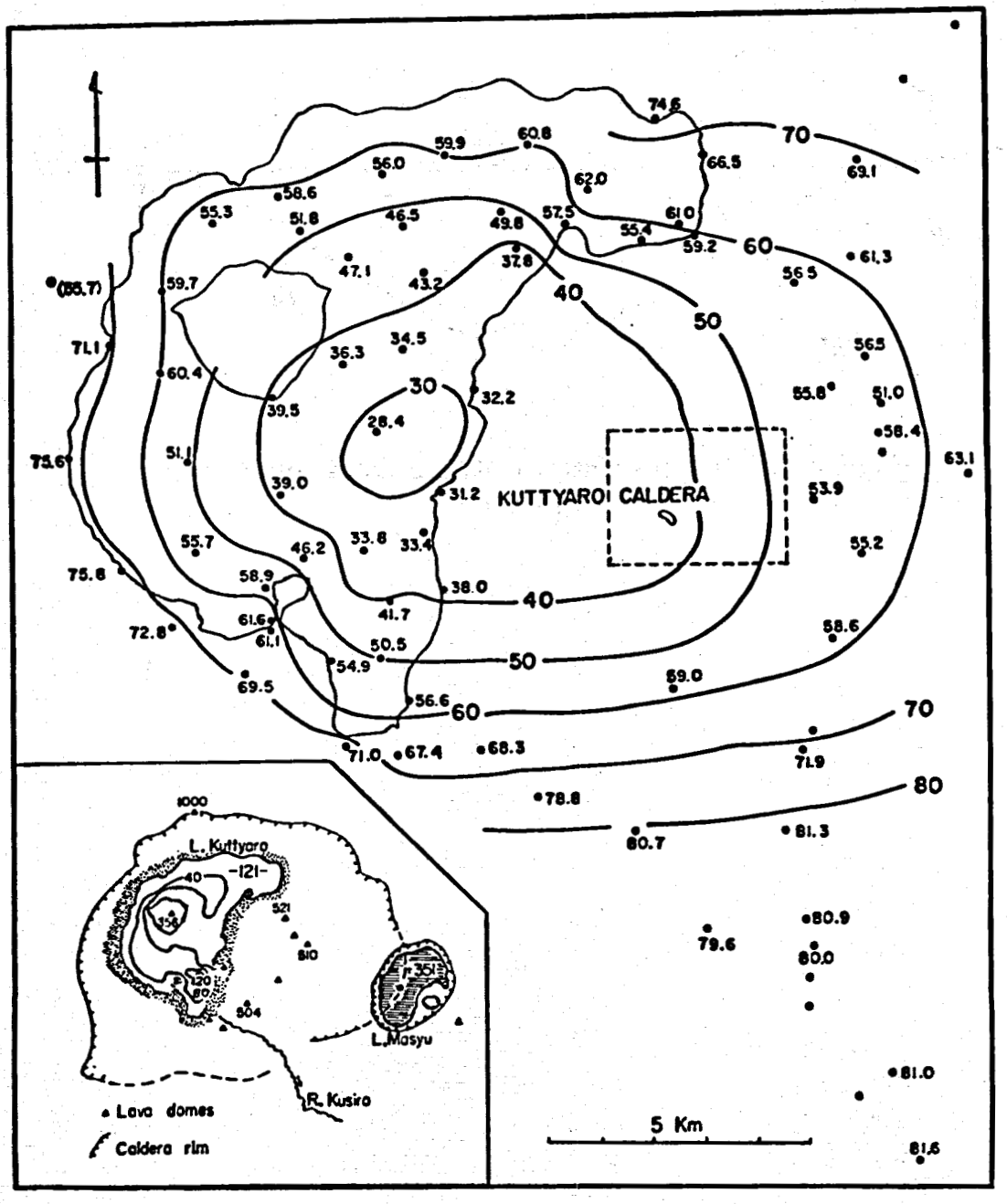

Figure 15. Distribution of Bouguer gravity anomalies on Kuttyaro Caldera. Unit is mgal

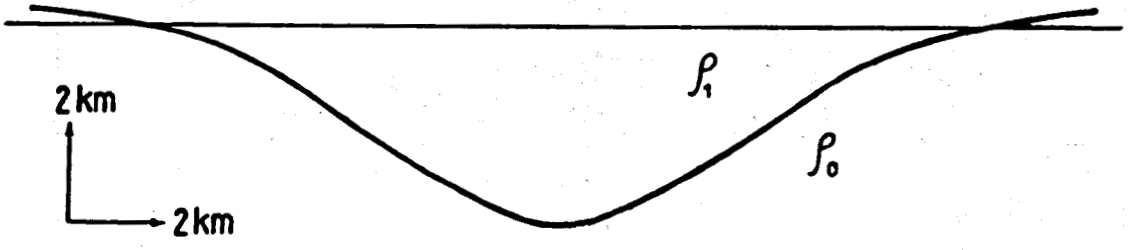

Figure 16. A schematic profile of Kuttyaro Caldera.
$\rho_0 - \rho_1 = 0.3$ g/cc

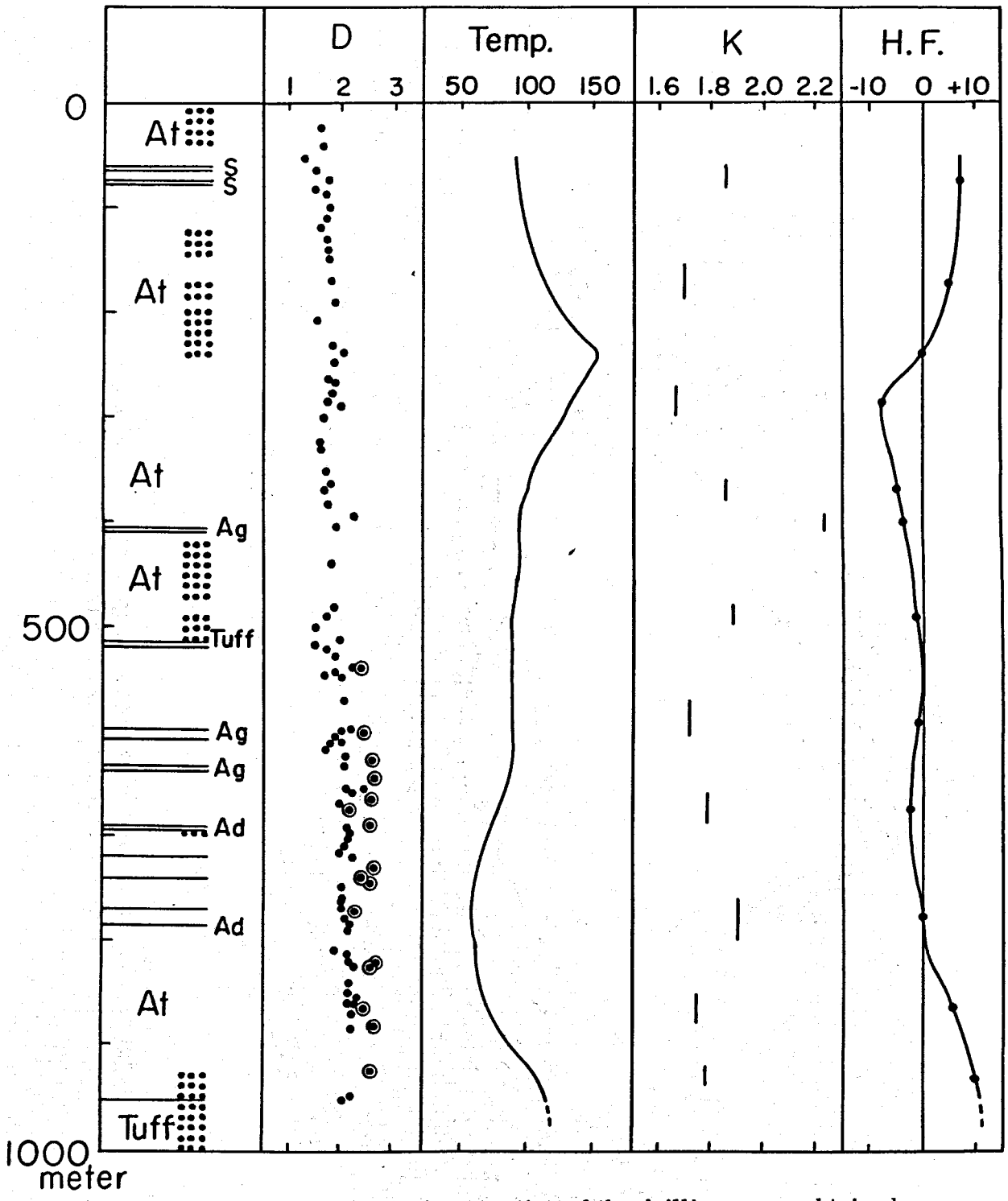

Figure 17. Some physical properties of the drilling cores obtained at Kuttyaro Caldera.

D: density (g/cc), Temperature (°C), K: thermal conductivity (X 10^{-3} cal/cm sec °C), H.F.: heat flow (X 10^{-6} cal/cm^2 sec), At: agglomerate tuff, S: sand stone, Ag: agglomerate, Ad: andesite. Double circles denote lava gragments

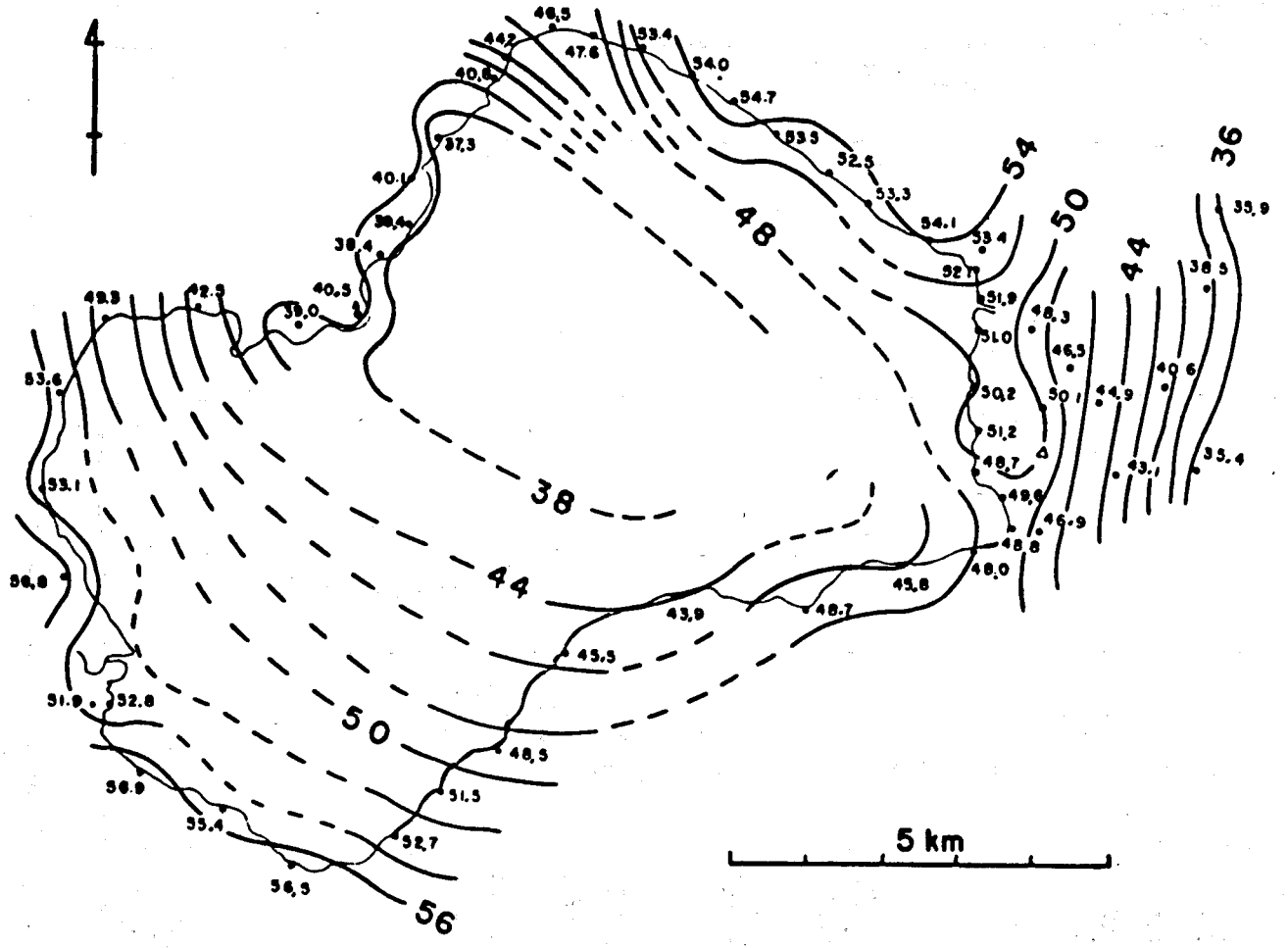

Figure 18. Distribution of Bouguer gravity anomalies on Sikotu Caldera. Unit is mgal

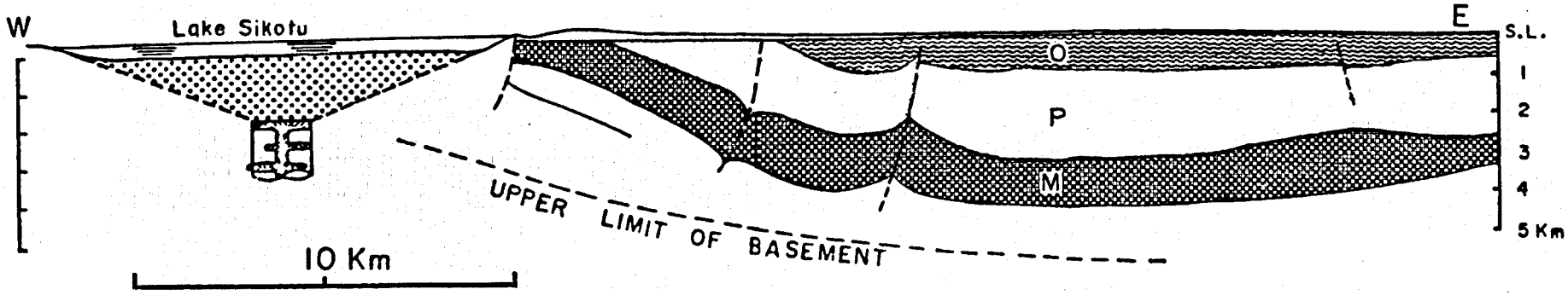

Figure 19. Schematic subsurface structure of Sikotu Caldera and vicinity.

Q: Quaternary, P: Pliocene, M: Miocene